J. Phys. B: Atom. Molec. Phys., Vol. 7, No. 8, 1974. Printed in Great Britain. © 1974

# Absolute cross sections for excitation of the $4^3$S, $3^3$P, and $4^3$D levels of helium by electron impact: Measurements at very low target-gas pressures

A F J van Raan†, P G Moll and J van Eck
Physics Laboratory, University of Utrecht, Utrecht, the Netherlands

Received 24 August 1973

**Abstract.** Total cross sections for electron-impact excitation of helium to the $4^3$S, $3^3$P, and $4^3$D-levels have been determined. From spectral line-intensity measurements we determined cross sections as a function of electron-impact energy $E_{el}$ (100–1000 eV) in the helium pressure region from $3\times10^{-5}$ to $3\times10^{-3}$ Torr. In the evaluation of the excitation cross sections polarization of the emitted radiation and cascade is taken into account. Special attention is paid to cascade from directly excited $n$F-levels which do not have well defined multiplicities. Pulse-counting techniques and automatic data-handling were necessary in order to measure the very low light-intensities with reasonable statistics. Only cross sections measured at the lowest target-gas pressures were used to evaluate excitation cross sections. The resulting excitation functions which may be attributed to exchange excitation show the following energy dependences for $E_{el} > 100$ eV without (between parentheses with) cascade corrections: $4^3$S, $E_{el}^{-2\cdot50}$ ($E_{el}^{-2\cdot46}$); $3^3$P, $E_{el}^{-2\cdot85}$ ($E_{el}^{-2\cdot90}$); $4^3$D, $E_{el}^{-2\cdot80}$ ($E_{el}^{-2\cdot75}$).

As far as the energy dependences are concerned, the experimental cross sections for $3^3$P- and $4^3$D-excitation are close to Ochkur's prediction, for the $4^3$S excitation the agreement is less. The experimental absolute cross sections for $4^3$D excitation are about an order of magnitude larger than those predicted by Ochkur.

Our work shows good agreement with very recent experimental work of Anderson *et al.*

## 1. Introduction

Because of the validity of Russell–Saunders coupling in helium (at least for S, P, and D levels), the electron-impact excitation of triplet levels from the ground state can virtually be attributed to electron exchange. Total cross sections for the process of electron exchange may therefore be determined from measurements of spectral lines, resulting from electron-impact excitation of helium triplet levels. This 'optical method' is hampered by serious experimental problems: such as the rapid decrease of line intensities as a function of energy and the (pressure dependent) influence of collisional transfer of excitation energy.

The experimental results so far show large mutual differences. St John *et al* (1964), Moustafa Moussa *et al* (1967, 1969), and our group (van Raan *et al* 1971) published cross sections, measured at $5\times10^{-3}$, $10^{-3}$ and $5\times10^{-4}$ Torr, respectively. It turns out that the lower the target-gas pressure is, the lower the measured cross sections are. Therefore, it seems more appropriate to regard these above results as apparent cross-sections at the pressure mentioned, rather than as 'pure exchange' cross sections.

† Present address: Faculty of Physics, University of Bielefeld, Viktoriastrasse 44, Bielefeld, W. Germany.

Recently, Kay and Showalter (1971) published the results of optical measurements at a target-gas pressure of $10^{-3}$ to $10^{-2}$ Torr. They interpreted their results with help of a model for collisional transfer (St John and Fowler 1961) of excitation energy in order to correct for the pressure-dependent effect. Very recently, Anderson *et al* (1973) published results of $4^3$S and $3^3$P excitation. For the case of $3^3$P, their results disagree considerably with the results of Kay and Showalter (1971) but agree quite reasonably with our results.

To perform measurements on triplet-level excitation which are as much as possible free from the influence of collisional transfer, it is necessary to work at sufficiently low target-gas pressures. In that case, apparent cross sections which are practically independent of pressure should be found. In some cases (at higher electron-impact energies for the $3^3$P and the $4^3$D-level) it turned out to be impossible to measure apparent cross sections independent of pressure because of the very small electron-impact excitation cross sections. Plotting apparent cross sections against pressure (both on linear scales) one has, in principle, a curve increasing at low pressures (linear at very low pressures) due to the effect of collisional transfer. When the electron-impact cross sections are large enough, the slope of such a curve will be virtually zero and one generally speaks about 'pressure independent'. We shall use this expression in the same sense, referring to the relevant figures in §§ 4.1, 4.2 and 4.3. In the cases we were not able to measure in the 'pressure-independent region' (especially at higher electron energies for $4^3$D) we applied a simple extrapolation using only the measurements at the lowest pressures, $5\times10^{-5} < p < 5\times10^{-4}$ Torr. At such a low pressure this procedure is completely reliable in order to obtain the apparent cross section at 'zero pressure'. All other experimental data (so, in general, the pressure dependences of all cross sections measured) were used for comparison with numerical calculations on the collisional-transfer problem.

## 2. Apparatus and experimental technique

In a vacuum chamber of stainless steel a system is mounted consisting of the electron source (a 3 mm diameter oxyd-cathode), the electron lenses (separated by glass spacers), the collision chamber (the field free 'measuring cage'), and the electron collector-cup (see figure 1). The collision chamber is a cylindrical tube (made of a vanadium–chromium alloy) with a diameter of about 3 cm and a length of about 2 cm. The target gas is introduced into the vacuum chamber via a needle valve. The light emitted upon excitation of the target gas by the collimated electron beam (no magnetic field was used) is observed through a slit parallel to the electron beam (length 1·5 cm, height 0·4 cm) in the cylindrical tube. In this way practically only the light caused by the beam electrons was observed. The length of the observed part of the beam is about 0·8 cm.

The vacuum chamber is connected to a 150 litre $s^{-1}$ diffusion pump, cooled by a liquid–air baffle. The background pressure is about $1\times10^{-7}$ Torr ($N_2$ equivalent). Pressures are measured with help of a Bayard–Alpert ionization gauge which is accurately calibrated in situ against a capacitance manometer (MKS Baratron type 170) in the pressure range $5\times10^{-5}-5\times10^{-3}$ Torr. The radiation produced by the excitation process, passing through the slit in the collision chamber and a window in the vacuum chamber is analysed by means of a Leiss monochromator. This monochromator (Czerny–Turner mounting) has a spectral range of 300–600 nm and is provided with an entrance slit (perpendicular to the electron beam) and plane Bausch and Lomb grating

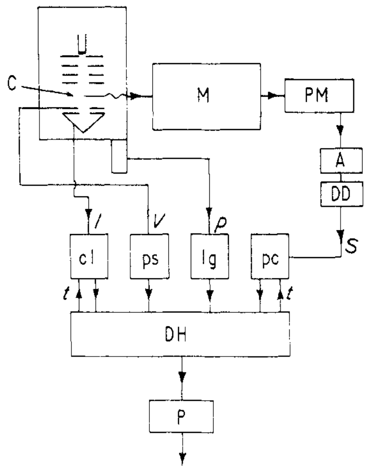


**Figure 1.** Block diagram of the apparatus. C collision chamber; M Leiss monochromator; PM photomultiplier; A amplifier; DD differential discriminator; PC puls counter; IG ionization gauge; PS power supply acceleration-voltage; CI current integrator; DH data-handling; P punching machine; $S$ signal; $p$ pressure (target gas, background); $V$ acceleration voltage; $I$ electron-beam current; $t$ adjustable time.

(1800 lines $mm^{-1}$). An EMI 6256 photomultiplier just behind the exit slit is used to detect the light of a selected spectral-line. For the present measurements we used slit widths of 0·5 mm and a slit height of 5 mm, so that the grating is entirely illuminated (in the direction parallel to the slit). The photomultiplier is cooled to about $-25\,°C$ by Peltier elements. The direction of observation is perpendicular to the electron beam.

Because of the low light-intensities (in some cases 1 or 2 pulses per second, the same as the background signal) counting techniques with automatic data-handling were used to measure the photomultiplier signal, together with the other necessary experimental parameters. Only in this way reasonable statistics could be obtained. In figure 1 a block diagram of the apparatus, including the data-handling system, is given. In each measuring-series the following parameters were measured: background pressure ($p_b$), working pressure ($p_w$), spectral line-intensity ($S_t$), background intensity ($S_b$) (which includes stray light, light resulting from excited background gases, photomultiplier noise), the electron-beam current collected by the cup ($I$), and the accelerating voltage of the collision chamber ($V$) (cathode at zero potential). This procedure was performed during an adjustable time and was repeated until good statistics were obtained. Measurements over a long period (eg one hour) divided in small time-intervals (eg ten seconds) were chosen in order to eliminate the influence of shortly lasting disturbances. A computer program, designed for the elaboration of the recorded data, eliminated the measuring series affected by disturbances by means of a statistical criterion. With help of this program (apparent) cross sections for the excitation of a given level were calculated (including calculation of the measuring accuracy) as a function of electron energy and of target-gas pressure.

The voltage on the electrode just before the collision chamber and on the collector cup was about 30 % higher than the accelerating voltage on the collision chamber. With this potential configuration secondary electrons were prevented from entering the collision chamber as well as possible. The performance of the electron beam was checked by monitoring the currents on the front and back plate of the collision chamber; these currents were always limited to at most 1% of the primary beam-current. With help of potential distribution measurements on a similar model of the electrode system, we verified that the above mentioned potential configuration did not influence the adjusted accelerating voltage in the collision chamber at the place of observation, see for example van Eck and de Jongh (1970) and de Jongh (1971).

## 3. Evaluation of the cross sections

### *3.1. Basic concepts*

The principle of optical studies of excitation processes is the determination of total cross sections from spectral line-intensity measurements. In the most simple case, population is achieved only by electron-impact excitation of just the level concerned. Depopulation takes place by radiative decay. Complications arise by cascade (population by radiative decay from higher excited levels), collisional transfer of excitation energy, and imprisonment of resonance radiation. This latter effect is of course important in the case of measurements on resonance levels. However, because resonance levels play a dominant role in the process of collisional transfer, imprisonment of resonance radiation is, especially at higher target-gas pressure ($p > 10^{-3}$ Torr), in many cases a nonnegligible effect. We shall give here an expression for excitation cross sections, derived from a balance equation between population and depopulation of a level. For the detailed derivation the reader is referred to Gabriel and Heddle (1960) and to van Raan (1974a).

For the case where it suffices to take only cascade resulting from electron impact into account, the cross section $\sigma_i$ for excitation from the ground state to level $i$ is given by (see, for example, van Raan 1974a):

$$\sigma_i = \sigma_{ij} \frac{\Sigma_{j(<i)} A_{ij}}{A_{ij}} - \sum_{h(>i)} \sigma_{hi}. \tag{1}$$

Here $\sigma_{ij}$ is the cross section for the production of photons $i \to j$, the so called *emission* or *optical* cross section, calculated from the line intensity $i \to j$; $A_{ij}$ is the probability for the spontaneous transition $i \to j$, therefore $(\Sigma_{j(<i)} A_{ij})^{-1} = \tau_i$ is the natural lifetime of level $i$. The factor $A_{ij}/(\Sigma_{j(<i)} A_{ij})$ is the branching ratio. The second term on the right-hand side represents the cascade contribution, expressed in emission cross sections.

The emission cross section $\sigma_{ij}$ is calculated from the experimental parameters as follows

$$\sigma_{ij} = \frac{4\pi}{\omega} \frac{S_{ij}}{Nk(\lambda_{ij})LI/e}. \tag{2}$$

$S_{ij}$ is the output signal (Coulombs s$^{-1}$) of the photomultiplier, resulting from the emission of radiation into the acceptance solid-angle $\omega$ (entrance slit area divided by the square of the distance between electron-beam and entrance slit); $N$ is the number density of the target gas; $I$ is the electron-beam current; $e$ is the charge of an electron (so $I/e$ is the number of projectile electrons passing per sec through a plane perpendicular to the beam); $L$ is the length of the observed part of the beam; $k(\lambda_{ij})$ is the quantum efficiency of the spectrometer (monochromator plus detector) *for unpolarized light*. In fact, the right-hand side of expression (2) has to be multiplied with an appropriate factor $P$ in order to take the *polarization* of the emitted radiation into account. This means, we have to find a relation between $S_{ij}/k(\lambda_{ij})$ and the average intensity of the radiation $i \rightarrow j$. We will discuss this further in § 3.4.

When collisional transfer is not negligible (at higher target-gas pressures) the expression for the excitation cross section is rather complicated. In fact a pressure dependent apparent cross section is found. We again refer to Gabriel and Heddle (1960) and to van Raan (1974a).

### 3.2. Treatment of data; absolute values

Relative apparent cross sections are derived with the aid of expression $S_{ij}/pI$. The spectrometer signal $S_{ij}$ is corrected for background intensity, $S_{ij} = S_t - S_b$, as given in § 2. The target-gas pressure is found by $p = p_w - p_b$.

For the evaluation of absolute cross sections it is in principle necessary to know also the remaining parameters in equation (2): $\omega$, $L$, and $k(\lambda_{ij})$. However, we performed the present measurements with the same optical equipment and the same direction of observation as in our earlier work (van Raan *et al* 1971). Therefore we normalized our relative measurements to the results of this work. We first checked the variation of the relative spectrometer-quantum-efficiency with wavelength. The ratios of a number of spectral line-intensities ($4^1S \rightarrow 2^1P$, 504·8 nm, $4^1D \rightarrow 2^1P$, 492·2 nm, $3^1P \rightarrow 2^1S$, 501·6 nm, $4^3S \rightarrow 2^3P$, 471·3 nm, $3^3P \rightarrow 2^3S$, 388·9 nm) were determined at 200 eV in one measuring-series and then compared with the same ratios resulting from our earlier work. The differences were at most 7% at random; this is within the measuring error.

### 3.3. Check of experimental conditions

In order to check the experimental conditions of our apparatus (the linearity of the detecting system) and as a check on the absence of multiple scattering of the primary electrons we investigated the proportionality of the (background corrected) signal with the electron-beam current, $I$, at a constant pressure of $1{\cdot}5 \times 10^{-4}$ Torr (figure 2(*a*)) and with the target-gas pressure, $p$, at a constant beam-current of 200 μA (figure 2(*b*)). For this purpose we used the $4^1S \rightarrow 2^1P$ transition, especially because of the second point: the apparent cross section for the $4^1S$ level is 'pressure independent', at least for $p < 2 \times 10^{-3}$ Torr. The results given in figure 2 show a proportionality of the signal with $I$ and $p$ till at least 400 μA and $2 \times 10^{-3}$ Torr, respectively. Only at high electron-impact energies (800–1000 eV) beam currents of about 350 μA were used. At lower energies lower currents (at 100 eV about 50 μA) were used, particularly in order to diminish the influence of space-charge effects (distortion of energy scale).

All measurements were performed in the pressure region $3 \times 10^{-5}$ to $3 \times 10^{-3}$ Torr. A check on the linearity of the ionization gauge, as well as an absolute calibration of this gauge was performed in situ with a capacitance manometer.

### 3.4. Polarization of the emitted radiation

Radiation emitted by atoms excited by an unidirectional electron beam is, in general, polarized. This is due to the fact that the angular momentum transferred by the electron to the target-gas atoms will have a certain preferential direction. This effect introduces an asymmetry in the population of the different magnetic substates and, consequently, a polarization and anisotropic distribution of the emitted radiation (Percival and Seaton

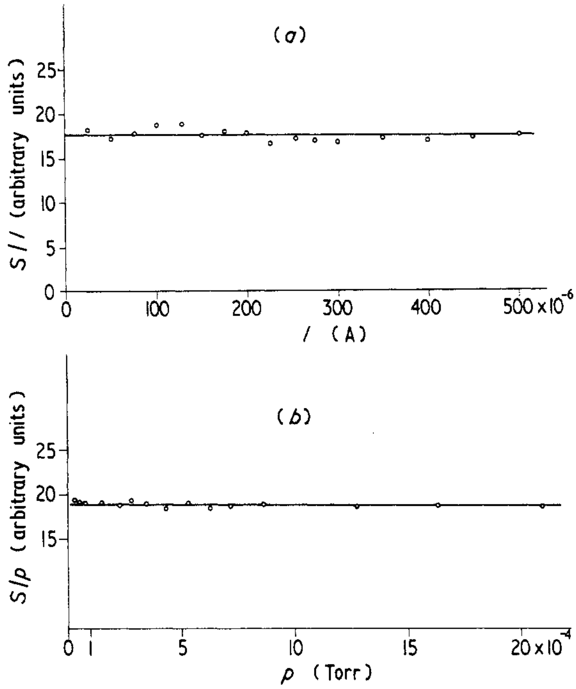


**Figure 2.** (*a*) Line intensity signal $S$/electron-beam current $I$, as a function of $I$ at a constant target-gas pressure of $1{\cdot}5 \times 10^{-4}$ Torr ($4^1S \rightarrow 2^1P$ line intensity, $E_{el} = 400$ eV). (*b*) Line intensity signal $S$/target-gas pressure $p$, as a function of $p$ at a constant electron-beam current of 200 μA ($4^1S \rightarrow 2^1P$ line intensity, $E_{el} = 400$ eV).

1958). Therefore, measuring spectral line-intensities (resulting from electron impact) under a special observation angle, one has to take these effects into account in order to evaluate total cross sections. Further, the polarization degree of the emitted radiation is dependent upon the energy of the projectile electrons and the target-gas pressure.

It is possible to avoid polarization effects by the use of a polaroid in a specific way (Clout and Heddle 1969a and 1969b) or by observation of the electron-beam under the magic angle (De Jongh and Van Eck 1971, De Jongh 1971). Both methods however, have some disadvantages in the case of our experiment. The use of a polaroid would mean a loss of intensity of at least 35%. Because of the very low line-intensity we could not afford such a loss. Placing the electron beam under the magic angle (in fact a combination of two specific angles) would require a new absolute intensity calibration; we preferred to use our earlier calibration results (van Raan *et al* 1971) which appeared to be reasonable. Further, in the case of the magic angle set-up the acceptance solid angle would be considerably smaller. Hence also a loss of intensity would be involved. Therefore we did not perform 'polarization free' measurements, the more because it appeared that in connection with the apparatus polarization the eventual polarization correction-factor would not differ drastically from unity.

The polarization degree $\Pi$ of the emitted radiation and the polarization degree $P_s$ of the spectrometer are defined as, respectively:

$$\Pi = \frac{I_{\parallel} - I_{\perp}}{I_{\parallel} + I_{\perp}} \qquad P_s = \frac{k_{\parallel} - k_{\perp}}{k_{\parallel} + k_{\perp}} \tag{3}$$

where $I_{\parallel}$ and $I_{\perp}$ are the intensities of the radiation components with the electric vector parallel and perpendicular to the electron beam, respectively. The observation angle $\phi$ (angle between the electron beam and the direction of observation) is 90°.

One may show (Van den Bos *et al* 1968) that for the case of electric-dipole radiation and an observation angle $\phi = 90°$ the complete polarization-correction factor (in order to evaluate total cross sections) is given by

$$P = \frac{(B+1)(C+2)}{3(BC+1)}$$

where (4)

$$B = \frac{1+P_s}{1-P_s} \qquad C = \frac{1+\Pi}{1-\Pi}.$$

With this expression the right-hand side of equation (2) should be multiplied in order to find the correct value for the total emission cross section.

We shall use polarization-correction factors $P$ calculated from experimental polarization degrees (Heddle and Lucas 1963) and with help of our instrumental polarization.

### 3.5. *Corrections for cascade*

By the concept cascade we understand in principle all modes of radiative decay from higher levels towards the levels studied. In this work it is important to distinguish between cascade resulting from levels excited by collisional-transfer processes and cascade resulting from levels excited by electron impact. For the evaluation of excitation cross sections only data from measurements in a 'pressure-independent region' or from an extrapolation to zero pressure are used. It is clear, that then only the second 'kind' of cascade is involved. Therefore, in the case of triplet levels, only cascade from higher triplet levels, excited by electron-impact (exchange) excitation, will contribute.

However, a complication arises due to the F-levels. Breakdown of Russell–Saunders coupling introduces a mixed multiplicity. So, when 'singlet' F-levels are excited by direct electron-impact, a triplet character will also be present (Parish and Mires 1971 and Van den Eynde *et al* 1972). The energy dependence of the cascade from these triplet F-levels will reflect the energy dependence for excitation of singlet F-levels. According to the Born–Bethe approximation for collision-induced optically forbidden transitions this energy dependence decreases, for sufficiently high electron-impact energies, as $E_{el}^{-1}$. Therefore, Kay and Showalter (1971) corrected their experimental results by subtracting a '$E_{el}^{-1}$-component' from their 'to zero pressure extrapolated' experimental data. We shall discuss this further in §§ 4.2 and 4.3. The cascade contribution from directly-excited mixed F-levels is, of course, of immediate importance for the $n^3$D-levels; $n^3$S and $n^3$P-levels are indirectly affected through intermediate cascade-steps (via the $n^3$D-levels). The experimental results support this reasoning.

In the 'pressure-independent' region the apparent cross section $\sigma_i'$ is simply given by equation (1) with

$$\sigma_{hi} = A_{hi}\tau_h\sigma_h'$$

so that

$$\sigma_i' = \sigma_i + \sum_{h(>i)} A_{hi}\tau_h\sigma_h'. \tag{5}$$

We further write for the branching ratio $A_{hi}\tau_h = \beta(h \to i)$. Of course, in $\sigma'_h$ again cascade (to levels $h$) is involved. For the levels studied in this work we now may write

$$\sigma'(4^3\text{S}) = \sigma(4^3\text{S}) + \sum_{n^3\text{P}(>4^3\text{S})} \beta(n^3\text{P} \to 4^3\text{S})\sigma'(n^3\text{P}) \tag{6a}$$

$$\sigma'(3^3\text{P}) = \sigma(3^3\text{P}) + \sum_{n^3\text{S}(>3^3\text{P})} \beta(n^3\text{S} \to 3^3\text{P})\sigma'(n^3\text{S}) + \sum_{n^3\text{D}(>3^3\text{P})} \beta(n^3\text{D} \to 3^3\text{P})\sigma'(n^3\text{D}) \tag{6b}$$

$$\sigma'(4^3\text{D}) = \sigma(4^3\text{D}) + \sum_{n^3\text{P}(>4^3\text{D})} \beta(n^3\text{P} \to 4^3\text{D})\sigma'(n^3\text{P}) + \sum_{n\text{F}(>4^3\text{D})} \beta(n^3\text{F} \to 4^3\text{D})\mu_n\sigma'(n^1\text{F}). \tag{6c}$$

(Cascade from $n$F-levels to $3^3$P via higher triplet D-levels is included in the apparent cross sections $\sigma'(n^3\text{D})$, see equation (6*b*)). In equation (6*c*) $\mu_n$ is a factor related to the mixing coefficients (Van Raan 1974a, Parish and Mires 1971, Van den Eynde *et al* 1972). We further neglect exchange excitation of $n$F-levels compared with direct excitation. (Therefore we indicate $n^1$F). In the evaluation of $\sigma(4^3\text{D})$ no cascade correction is made for the third term at the right hand side of equation (6*c*). Therefore, we here accept $n$F-cascade as a special feature of the $4^3$D-excitation function and we shall apply only corrections for cascade contributions from higher triplet P-levels.

In order to calculate the cascade contributions from higher triplet levels, we need the cross sections concerned. The problem now is that these cross sections are hardly known, in fact our work is just mentioned to measure cross sections for some important triplet levels. The only way to make reasonable estimations of the cascade contributions is to scale our experimental cross sections to the values for the levels with higher principle quantum numbers $n$. A well-known scaling rule (Ochkur and Petrunkin 1963) is given by $n^{-3}$. Of course, this rule is only pertinent to *excitation* cross sections. In calculations of cascade contributions however, we need in fact *apparent* cross sections because the cascading levels will, in their turn, also be populated by cascade. Making the assumption that the percentage of cascade will not vary drastically with $n$, we may apply in reasonable approximation the afore mentioned scaling rule to our experimental apparent cross sections (at zero effective pressure). Therefore, we scaled the measured $\sigma'(4^3\text{S})$, $\sigma'(3^3\text{P})$, and $\sigma'(4^3\text{D})$ with the help of the $n^{-3}$ rule to $\sigma'(n^3\text{S})$, $\sigma'(n^3\text{P})$, and $\sigma'(n^3\text{D})$ respectively. It appeared that calculations up till $n = 15$ are sufficient.

We scaled $\sigma'(4^3\text{D})$ also in the energy range where $n$F-cascade dominates, again under the assumption that for each $n^3$D-level the relative amount of $m\text{F}(m > n)$-cascade will not change much. The outlined procedure is correct because we apply cascade corrections only at zero pressure ($p = 0$) so that the $n$F-contribution to the $4^3$D apparent cross section is not affected by ($P \to F$) collisional transfer. This procedure is important for the eventual cascade-correction for $3^3$P. May be a scaling with $n^{*-3}$ ($n^*$ is the effective principle quantum-number) would be more appropriate in order to calculate the cascade contributions (Gabriel and Heddle 1960). However, the difference with $n^{-3}$ scaling is only small. Because S-levels show the largest quantum defect, we calculated the cascade from S-levels towards $3^3$P (second term of the left hand side of equation (6b)) with $n^{*-3}$ scaling and compared this with the results for $n^{-3}$ scaling. The difference is only 4% ($n^{*-3}$ scaling gives the lowest values). We feel that the cascade corrections applied as outlined above are only approximative, but, it is the only way. Therefore, we shall present our experimental results both *without* any cascade correction and *with* the cascade corrections as outlined above.

## 4. Interpretation and discussion of the results

### *4.1. $4^3S$ level*

Detailed measurements were performed on the $4^3S \rightarrow 2^3P$ line at 471·3 nm. Figure 3(*a*) shows the apparent cross sections for the $4^3S$ level at 200, 300, 400 and 500 eV measured in the pressure region $3 \times 10^{-5} - 3 \times 10^{-3}$ Torr. These pressure-dependence curves for the different electron-impact energies are composed of 5 to 10 separate measuring series. Because of the good statistics, the accuracy of the results is rather high; mean random errors of less than 10% per measuring point are to be expected for all impact energies and target-gas pressures. In order to put the pressure-dependence curves of all energies measured at one scale, we performed energy-dependence measurements at $3 \times 10^{-4}$ Torr. At this target-gas pressure the apparent cross sections are virtually 'pressure independent' for all electron-impact energies considered.

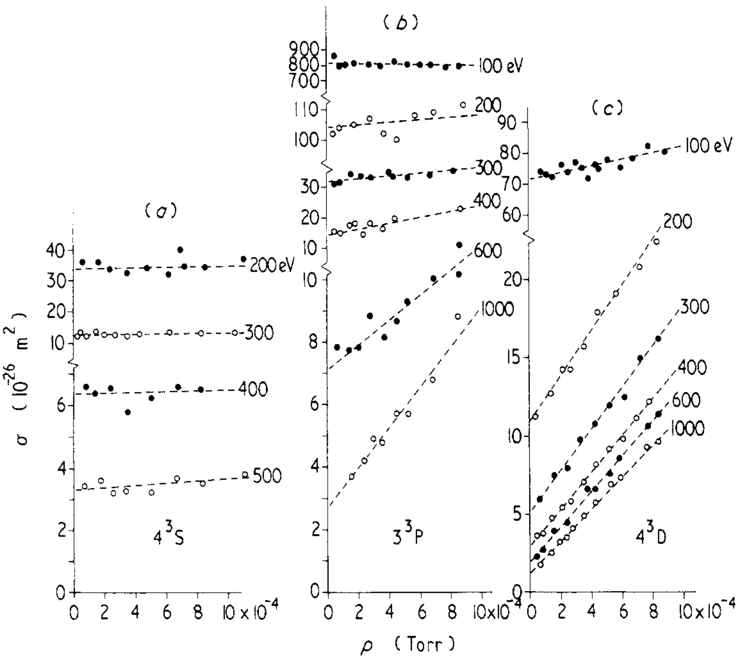


**Figure 3.** Absolute apparent cross sections for excitation (by electron impact) of helium to (*a*) $4^3S$; (*b*) $3^3P$ and (*c*) $4^3D$ as a function of target-gas pressure, at different electron-impact energies.

In the evaluation of the $4^3S$-excitation cross sections no polarization problems are encountered. The cascade corrections amount to at most 18%. These corrections are a function of electron-impact energy and therefore affect the energy-dependence of the uncorrected cross sections. The result is shown in figure 4(*a*) in a lg–lg plot; the numerical values are presented in table 1, together with the cascade contributions (see § 3.5). Absolute values are obtained by accurate normalization on the results of our earlier work, see § 3.2.

Because of the good statistics during the measurements, the absence of polarization corrections and the rather small cascade contributions, we believe that our *relative* measurements, which are directly pertinent to the energy dependence of the excitation (exchange) cross sections, are of high accuracy. The accuracy of the *absolute* values depends entirely upon the calibration procedure (van Raan *et al* 1971); here we may expect errors of about 15%, mainly due to the uncertainty in the absolute pressure measurement. We find that for energies larger than 100 eV the (electron-exchange) excitation cross section for the $4^3$S level decreases with $E_{el}^{-2\cdot50\pm0\cdot05}$ for the experimental data *without* any cascade correction and $E_{el}^{-2\cdot46\pm0\cdot05}$ *with* cascade correction. This is in disagreement with all known theoretical calculations: Ochkur (1964) predicts $E_{el}^{-3}$, Mott and Massey (1946) mention $E_{el}^{-2}$, Bell *et al* (1966) find approximately $E_{el}^{-3\cdot6}$ for the $2^3$S level. There is also no agreement with the experimental results of Kay and Showalter (1971); they found a slope of $-3\cdot0\pm0\cdot2$. However, this slope was determined by inclusion of data at 50 and 60 eV. These data have a high weight in their determination of the slope. Taking Kay and Showalter's data above 100 eV (as tabulated in their table 2) one obtains a slope of approximately $-2\cdot6\pm0\cdot1$ which is close to our result. Very recently, Anderson *et al* (1973) found $-2\cdot8\pm0\cdot2$, which is just between our result and Ochkur's prediction, with an error-bar overlap to both. Vriens *et al* (1968) found after integration of differential cross sections a slope of about $-3$ (between 100 and 225 eV) for the $2^3$S level. See table 2 for comparison of our experimental data with Ochkur's results; the agreement is quite good with respect to the absolute values.

All above mentioned theoretical calculations are based on the first Born-approximation. Bonham (1972) recently showed that second Born terms may play an important role in exchange excitation; he performed detailed calculations on second Born zero-angle differential cross sections for the $1^1\text{S} \rightarrow 2^3\text{S}$ and $1^1\text{S} \rightarrow 2^3\text{P}$ transitions.

### 4.2. $3^3$P-*level*

Detailed measurements were performed on the $3^3\text{P} \rightarrow 2^3\text{S}$ line at 388·9 nm. In figure 3(*b*) apparent cross sections for the $3^3$P-level at 100, 200, 300, 400, 600 and 1000 eV in the pressure region $3\times10^{-5}-2\times10^{-3}$ Torr are shown. Special care was taken in the evaluation of the cross sections because of the strongly wavelength-dependent background intensity due to $N_2$-excitation and straylight. Background intensities were measured at either side of the triplet line and compared with the background intensity at the centre of the triplet line's position in absence of the target gas. An intensity measurement just aside the nitrogen band but close to the triplet line gives, in presence of the target gas, an indication of the stray-light intensity. The computer program, suitable for the automatic data-handling, elaborated the different measurements in order to calculate accurate apparent cross sections. All data are collected in 5 to 10 separate measuring-series until good statistics were obtained.

We remark a stronger pressure dependence of the apparent cross sections than in the case of the $4^3$S level. Till 400 eV we were able to perform measurements in a nearly 'pressure-independent' region. Data at higher electron-impact energies are obtained by a simple extrapolation from the measuring points at the lowest pressures measured ($5\times10^{-5} < p < 5\times10^{-4}$ Torr) as discussed in § 1. The resulting excitation function is given in figure 4(*b*); numerical values are given in table 1. Because we are dealing with the electron-impact excitation of a non-S level, the experimental data have to be corrected for polarization of the emitted radiation. We used polarization degrees ($\Pi$) measured by Heddle and Lucas (1963). They measured $\Pi$ as a function of electron-impact energy at

$5 \times 10^{-4}$ Torr. We measured the energy dependence of the $3^3$P apparent cross sections at about the same target-gas pressure.

Because $\Pi$ is also a function of pressure, as mentioned in § 3.4, we may speak about an 'apparent $\Pi$' at a certain target-gas pressure. Apparent cross sections have to be corrected for an apparent $\Pi$ at the *same* pressure. The procedure in order to find the energy dependence from 100 eV at zero effective pressure is as follows. The energy dependence measured at $5 \times 10^{-4}$ Torr (reasonable light intensity, not too high target-gas pressure) was corrected to the energy dependence at zero effective pressure with help of the pressure-dependence measurements (see figure 3(*b*)). This means that the apparent cross sections at $5 \times 10^{-4}$ Torr ($\sigma'$(at $5 \times 10^{-4}$ Torr)) are to be multiplied with the factor $\sigma'$(at zero effective pressure)/$\sigma'$(at $5 \times 10^{-4}$ Torr) (see figure 3(*b*)). Both apparent cross sections have been corrected for the apparent $\Pi$ at the appropriate pressure. For $E_{\text{el}} < 300$ eV the polarization degree will not change any more below $p = 5 \times 10^{-4}$ Torr (see, for example, figure 5 of Heddle and Lucas). For these impact energies we therefore used $\Pi$ measured at $5 \times 10^{-4}$ Torr also at zero effective pressure. For $E_{\text{el}} > 300$ eV it seems plausible, according to the results of Heddle and Lucas, to use an apparent $\Pi = 0$ for $p = 5 \times 10^{-4}$ Torr. At these high electron-impact energies and pressure region collisional transfer introduces a strong depolarization. At zero effective pressure, it is quite possible that for $E_{\text{el}} > 300$ eV we are dealing with a negative polarization degree. From the measurements of Heddle and Lucas one may expect that $\Pi$ goes through zero at about 300 eV. There is no reason to believe that $\Pi$ will remain zero for higher impact energies. According to Bethe (1933) a constant negative polarization degree is to be expected for sufficiently high electron-impact energies. This polarization degree is given by:

$$\Pi_{\infty} = -\frac{\Pi_0}{2 - \Pi_0} \tag{7}$$

where $\Pi_0$ is the threshold polarization degree. For $3^3$P $\Pi_0 = 0{\cdot}37$ and thus $\Pi_{\infty} = -0{\cdot}22$. Therefore we may expect that for $E_{\text{el}} > 300$ eV the polarization degree at zero effective pressure will have a value between 0 and $-0{\cdot}22$. Further, cascade will lower the polarization degree. Especially for $E_{\text{el}} > 600$ eV there is a perceptible cascade contribution which can be attributed to cascade from F-levels via triplet D-levels. In the limiting case ($\Pi_{\infty} = -0{\cdot}22$) we find $P = 0{\cdot}94$ ($B = 0{\cdot}230$ for 388·9 nm, $3^3\text{P} \rightarrow 2^3\text{S}$).

Because of the uncertainties in the polarization degree, it is plausible to use $P = 1$ for the measured apparent cross sections above 300 eV at zero effective pressure. The polarization degrees and correction factors applied are presented in table 1. The polarization has only a small influence on the energy dependence of the uncorrected cross sections. In table 1 also cascade contributions are given. Cascade corrections have to be applied after correction for polarization. As may be noticed, cascade corrections amount to about 40–50% in the energy region where *n*F-cascade (via triplet D-levels) starts to dominate. In the energy range 100–600 eV we found a slope (energy dependence of the cross sections in a lg–lg plot) of $-2{\cdot}85 \pm 0{\cdot}10$ for the experimental data *without* any cascade correction and $-2{\cdot}90 \pm 0{\cdot}10$ *with* cascade correction. This is in notable agreement with Ochkur's theory. Mott and Massey (1946) mention $-3$, Bell *et al* (1966) find about $-3{\cdot}2$ for the $2^3$P level. However, according to Bonham (1972) second Born terms may play an important role in the calculation of total exchange cross sections for $3^3$P. There is also a good agreement between our absolute values and the results of Ochkur and Brattsev (1965), see table 2.

**Table 1.** Absolute cross sections for excitation of helium by electron impact

| eV | $4^3S$ | | | | | | $3^3P$ | | | | | | $4^3D$ | | | | | |
|---|---|---|---|---|---|---|---|---|---|---|---|---|---|---|---|---|---|---|
| | $\sigma_e$ | $\sigma_c$ | % | $\sigma$ | $\pi$ | $P$ | $\sigma_e$ | $\sigma_c$ | % | $\sigma$ | $\pi$ | $P$ | $\sigma_e$ | $\sigma_c$ | % | $\sigma$ | $\pi$ | $P$ |
| 100 | 2·00 | 0·359 | 18·0 | 1·641 | — | 1 | 6·99 | 1·91 | 27·3 | 5·08 | 0·188 | 1·062 | 0·74 | 0·179 | 24·2 | 0·561 | ~0 | ~1 |
| 150 | 0·685 | 0·113 | 16·5 | 0·572 | — | 1 | 2·07 | 0·68 | 32·9 | 1·39 | 0·140 | 1·045 | 0·235 | 0·056 | 23·8 | 0·179 | ~0 | ~1 |
| 200 | 0·345 | 0·050 | 14·5 | 0·295 | — | 1 | 0·964 | 0·32 | 33·2 | 0·644 | 0·088 | 1·026 | 0·103 | 0·025 | 23·1 | 0·078 | ~0 | ~1 |
| 250 | 0·196 | 0·026 | 13·3 | 0·170 | — | 1 | 0·551 | 0·19 | 34·5 | 0·361 | 0·039 | 1·012 | 0·0580 | 0·013 | 22·4 | 0·0440 | ~0 | ~1 |
| 300 | 0·127 | 0·016 | 12·6 | 0·111 | — | 1 | 0·323 | 0·12 | 37·2 | 0·203 | ~0 | ~1 | 0·0530 | 0·0078 | 14·7 | 0·0452 | ~0 | ~1 |
| 400 | 0·0636 | 0·0069 | 10·8 | 0·0567 | — | 1 | 0·146 | 0·067 | 45·9 | 0·0790 | ~0 | ~1 | 0·0300 | 0·0034 | 10·8 | 0·0266 | ~0 | ~1 |
| 500 | 0·0341 | 0·0037 | 10·8 | 0·0304 | — | 1 | 0·086 | 0·042 | 48·8 | 0·0334 | ~0 | ~1 | | | | | | |
| 600 | | | | | | | 0·074 | 0·030 | 40·5 | 0·0440 | ~0 | ~1 | 0·020 | 0·0011 | 5·5 | 0·0189 | ~0 | ~1 |
| 800 | | | | | | | 0·0305 | 0·018 | 59·0 | 0·0125 | ~0 | ~1 | 0·018 | 0·00048 | 2·7 | 0·0175 | ~0 | ~1 |
| 1000 | | | | | | | 0·0290 | 0·012 | 41·4 | 0·017 | ~0 | ~1 | 0·012 | 0·00025 | 1·8 | 0·0118 | ~0 | ~1 |

Column '$\sigma_e$': experimental excitation cross sections including cascade (from higher triplet levels); in the case of $4^3D$ also from $n$F-levels. Units $10^{-24}$ m$^2$.
Column '$\sigma_c$': cascade contribution from higher triplet levels (not from mixed $n$F-levels in the case of $4^3D$). (Units $10^{-24}$ m$^2$.)
Column '%': cascade contribution relative to the values of $\sigma_e$ (first column).
Column '$\sigma$': experimental excitation cross sections corrected for cascade (from higher triplet levels) except for cascade from mixed $n$F-levels in the case of $4^3D$. Units $10^{-24}$ m$^2$.
Column '$\pi$': polarization degree used for the correction (see text in §§ 4.2 and 4.3) of the apparent cross sections at $3 \times 10^{-4}$ Torr.
Column '$P$': polarization correction factor as given by equation (4).

Again, no agreement is obtained with the experimental results of Kay and Showalter (1971). They found a slope $-3{\cdot}5 \pm 0{\cdot}2$ *after* subtraction of a slower component with slope $-1$ (attributed to cascade from mixed F-levels as we discussed before). When indeed a mixed F-level contribution is present, we may represent the excitation function for high impact-energies, say $E_{\mathrm{el}} > 100$ eV, as

$$\alpha E_{\mathrm{el}}^{-s} + \beta E_{\mathrm{el}}^{-1}. \tag{8}$$

(According to Kay and Showalter $s = 3{\cdot}5$). This means, as soon as the second term is of the same order of magnitude as the initially dominant term ($\alpha E_{\mathrm{el}}^{-s}$), the excitation function will exhibit a deviation from a straight line with slope $-s$. In the work of Kay and Showalter this deviation starts at about 200 eV; their measurements are corrected to 'zero pressure' by means of an extrapolation with help of a collisional-transfer model.

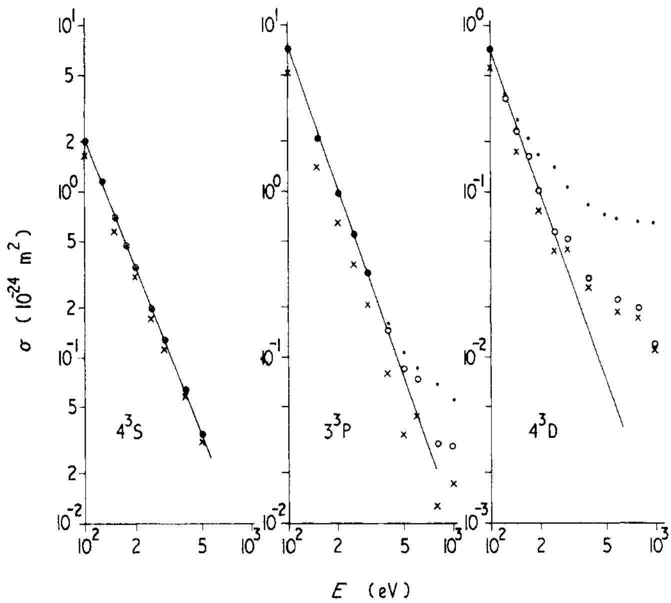


**Figure 4.** Absolute excitation cross sections of helium as a function of electron-impact energy. (*a*) the excitation function of $4^3$S; (*b*) the excitation function of $3^3$P; (*c*) the excitation function of $4^3$D. ● apparent cross sections at $3 \times 10^{-4}$ Torr for $4^3$S, at $5 \times 10^{-4}$ Torr for $3^3$P and at $3 \times 10^{-4}$ Torr for $4^3$D. ○ excitation cross sections at zero effective pressure, corrected for polarization but uncorrected for cascade. × excitation cross sections at zero effective pressure, corrected for polarization and for cascade.

This extrapolation appears to be in fact a linear one, but from relatively high pressures ($10^{-3}-10^{-2}$ Torr). Our measurements, which are performed practically at 'zero pressure', show the onset of a deviation from a straight line at about 500 eV. This difference between 'to zero extrapolated, data' (Kay and Showalter) and 'nearly at zero pressure measured data' (our work) is even more striking in the case of $4^3$D excitation. A nice agreement is obtained with the results of Anderson *et al* (1973). They obtained a slope of $-3{\cdot}0 \pm 0{\cdot}2$ (cascade-free results). We expect random errors in the cross sections as indicated in the plots (figures 3(*b*) and 4(*b*)), at most 15% for 1 keV. An inaccuracy in the absolute scale may introduce a systematic error of about 15%, as discussed in § 4.1.

### 4.3. $4^3$D-level

Measurements, performed on the $4^3D \rightarrow 2^3P$ transition at 447·1 nm, show much lower apparent cross sections *at very low pressures* than in the two foregoing cases. The apparent cross sections are very pressure dependent. Consequently, at higher pressures the line intensities for the different impact energies increase fast with pressure and at about $2 \times 10^{-3}$ Torr the line intensities are even of the same order of magnitude as in the case of $3^3P \rightarrow 2^3S$.

In fact only 100 eV was measured in a nearly 'pressure independent' region (see for the pressure-dependence curves figure 3(*c*)). The resulting excitation function is shown in figure 4(*c*); the values are tabulated in table 1. The excitation function was measured at $3 \times 10^{-4}$ Torr, all relevant data were corrected with the factor $\sigma'$(at $3 \times 10^{-4}$ Torr/$\sigma'$(at zero effective pressure). Reasonable statistics, especially at low target-gas pressures, were obtained by measuring a sufficiently long time, for example: five hours for the pressure-dependence curve at 1000 eV (about 25 measuring points). The excitation function given in the lg–lg plot, shows a slope of $-2{\cdot}8 \pm 0{\cdot}10$ (between 100 and 250 eV) for the experimental data *without* any cascade correction and $-2{\cdot}75 \pm 0{\cdot}10$ *with* cascade corrections (see further on in this section). In principle, polarization corrections are necessary for the $4^3$D levels. Heddle and Lucas measured $\Pi$ at $1 \times 10^{-3}$ Torr up till only about 80 eV. For these electron-impact energies the apparent cross section and also the polarization degree, is 'pressure independent' at $1 \times 10^{-3}$ Torr. An extrapolation of the measurements of Heddle and Lucas gives $\Pi = 0$ at about 100 eV. Theoretically (Bethe 1933) the polarization degree will decrease to a $\Pi_\infty$ value at sufficiently high energies (see equation (7)). In the case of $4^3$D the threshold polarization degree $\Pi_0 = 0{\cdot}317$ so that $\Pi_\infty = -0{\cdot}19$. However, such a polarization degree will only be valid at high electron energies (from, say, 400 eV). For these impact energies we were not able to find a 'pressure independent' region for the apparent cross section. At the pressures measured (see figure 3(*c*)) a strong depolarization introduced by collisional transfer of excitation energy will be present (see, for example, figure (5) of Heddle and Lucas). It is reasonable to take $\Pi = 0$ for $E_{el} > 100$ eV. This procedure will not introduce an appreciable error. Further, even at $p = 0$ the direct cascade will have a depolarizing effect. For example, the error made by taking $\Pi = 0$ instead of $\Pi = 0{\cdot}19$ amounts about 4% (apparatus polarization $B = 0{\cdot}27$ at 447·1 nm).

The cascade contributions pertinent to the apparent cross sections are given in table 1. As is to be seen, cascade corrections (aside from *n*F-levels) amount to at most 24%.

Kay and Showalter measured the $3^3$D level. We may expect that the $4^3$D-level will show a similar behaviour with regard to the pressure dependence. Their $3^3$D excitation function (given in a lg–lg plot) starts to deviate from a straight line attributed to exchange excitation $\alpha E_{el}^{-s}$ in equation (8)) already at about 60 eV. Our measurements, performed up till very low target-gas pressures, clearly yield, up to 250 eV, a straight line. Furthermore, there is no agreement between the slope resulting from our measurements ($s = -2{\cdot}80$) and from Kay and Showalter's experiment ($s = -3{\cdot}8$).

As in the case of $3^3$P, there is a notable agreement between our measured energy dependence and that predicted by Ochkur (1964); Mott and Massey (1946) mention $-4$. The absolute values are not in agreement with the Ochkur calculations, his absolute values are about an order of magnitude smaller than our experimental values (see table 2).

We expect random *relative* errors as indicated in the plots (figures 3(*c*) and 4(*c*)) at most 15% for the cross section at 1 keV (which is the value of the intersection of the pressure dependence curve ($p < 4 \times 10^{-4}$ Torr, $E_{el} = 1$ keV) with the ordinate, see figure 3(*c*). An inaccuracy in the absolute scale may introduce a systematic error of about 15%.

**Table 2.** Comparison with theoretical cross sections

| eV | $4^3$S | | | $3^3$P | | | $4^3$D | | |
|---|---|---|---|---|---|---|---|---|---|
| | $\sigma_e$ | $\sigma$ | $\sigma_{Ochkur}$ | $\sigma_e$ | $\sigma$ | $\sigma_{Ochkur}$ | $\sigma_e$ | $\sigma$ | $\sigma_{Ochkur}$ |
| 100 | 2·00 | 1·641 | 2·47 | 6·99 | 5·08 | 4·84 | 0·740 | 0·561 | 0·0634 |
| 150 | 0·685 | 0·572 | 0·775 | 2·07 | 1·39 | 1·41 | 0·235 | 0·179 | 0·0185 |
| 200 | 0·345 | 0·295 | 0·335 | 0·964 | 0·644 | 0·608 | 0·103 | 0·078 | 0·00801 |
| 300 | 0·127 | 0·111 | 0·097 | 0·323 | 0·203 | 0·185 | 0·0530 | 0·045 | 0·00238 |
| 400 | 0·0636 | 0·0567 | 0·0423 | 0·146 | 0·079 | 0·0766 | 0·0300 | 0·027 | 0·00106 |
| 500 | 0·0341 | 0·0304 | 0·0211 | 0·086 | 0·033 | 0·0396 | | | |

Columns '$\sigma_e$' and '$\sigma$' as given in table 1; column '$\sigma_{Ochkur}$': exchange-excitation cross sections calculated by Ochkur and Brattsev (1965). (Units $10^{-24}$ m$^2$.)

## 5. Conclusions

From our experimental work we may draw the following conclusions;

(i) The energy dependence of that part of the exciation functions which may be attributed to exchange excitation is close to Ochkur's prediction especially for the $3^3$P and $4^3$D-level. The largest discrepancy with Ochkur's work exist for the $4^3$S-level.

(ii) The largest discrepancy with Ochkur's work, with respect to the absolute cross section values, exists for the $4^3$D-level.

(iii) At electron-impact energies $>250$ eV the excitation function of the $4^3$D-level is dominated by an energy dependence other than one which may be attributed to exchange excitation. In connection with the character of this energy dependence it is plausible to attribute this part of the excitation function to predominantly cascade from directly excited F-levels which show, according to theoretical and experimental investigations, a mixing of multiplicity.

(iv) The pressure dependence of the apparent cross section shows at low pressures ($p < 10^{-3}$ Torr) a behaviour as is to be expected (linear with target-gas pressure). As an example the pressure dependence of the apparent cross sections of $4^3$D at several electron-impact energies between 200 and 1000 eV is shown in figure 3. The slopes of the straight lines through the measuring points should reflect the energy dependence of the excitation of $n^1$P-levels.

## Acknowledgments

The authors are grateful to Professor J A Smit and Dr H G M Heideman for valuable comments and stimulating remarks on the manuscript. They also express their thanks to Dr F J de Heer and Dr G Nienhuis for their continuous interest. Thanks are due to H J J van Vliet for taking part of the experimental data. For technical and computational assistance we are indebted to J van der Weg and K J Goslinga.

This work was performed as part of the research program of the 'Stichting voor Fundamenteel Onderzoek der Materie' (FOM, Foundation for Fundamental Research on Matter) financially supported by the 'Nederlandse Organisatie voor Zuiver Wetenschappelijk Onderzoek' (ZWO, Netherlands Organization for the Advancement of Pure Scientific Research).

## References

Anderson R J, Hughes R H, Tung J H and Chen S T 1973 *Phys. Rev.* A **8** 810–5
Bell K L, Eissa H and Moïseiwitsch B L 1966 *Proc. Phys. Soc.* **88** 57–63
Bethe H A 1933 *Handb. Phys.* **24** 508–15 (Berlin: Springer)
Bonham R A 1972 *J. chem. Phys.* **57** 1604–12
van den Bos J, Winter G J and de Heer F J 1968 *Physica* **40** 357–84
Clout P N and Heddle D W O 1969a *J. Opt. Soc. Am.* **59** 715–7
—— 1969b *J. Phys.* E: *Sci. Instrum.* **2** 929–30
van Eck J and de Jongh J P 1971 *Physica* **47** 141–58
—— 1971 *VII ICPEAC Amsterdam* 701–3
van den Eynde R K, Wiebes G and Niemeyer Th 1972 *Physica* **59** 401–18
Gabriel A H and Heddle D W O 1960 *Proc. R. Soc.* A **258** 124–45
Heddle D W O and Lucas C B 1963 *Proc. R. Soc.* A **271** 129–42
de Jongh J P and van Eck J 1971 *Physica* **51** 104–12
de Jongh J P 1971 *thesis* University of Utrecht
Kay R B and Showalter J G 1971 *Phys. Rev.* A **3** 1998–2005
Mott N F and Massey H S W 1946 *The Theory of Atomic Spectra* (Oxford: Clarendon Press)
Moustafa Moussa H R 1967 *thesis* University of Leiden
Moustafa Moussa H R, de Heer F J and Schutten J 1969 *Physica* **40** 517–49
Ochkur V I 1964 *Soviet Phys.-JETP* **18** 503–8
Ochkur V I and Brattsev V F 1965 *Opt. Spectrosc.* **19** 274–6
Ochkur V I and Petrun'kin A M 1963 *Opt. Spectrosc.* **14** 245–248
Parish R M and Mires R W 1971 *Phys. Rev.* A **4** 2145–60
Percival I C and Seaton M J 1958 *Phil. Trans. R. Soc.* A **251** 113–38
van Raan A F J, de Jongh J P, van Eck J and Heideman H G M 1971 *Physica* **53** 45–59
van Raan A F J 1973a *Physica* **65** 566–78
—— 1974a *J. Phys.* B to be submitted
St John R M and Fowler R G 1961 *Phys. Rev.* **122** 1813–20
St John R M, Miller F L and Lin C C 1964 *Phys. Rev.* **134** A 888–97
Vriens L, Simpson J A and Mielczarek S R *Phys. Rev.* **165** 7–15